Supporting Information

Impact of Vacancy Defects on the Thermal Conductivity of BaAgBi: A Comprehensive Study by Molecular Dynamics Simulations with Neural Network Potentials

Yunzhen Du[abc], Yuan Yao[ac] , Kunling Peng[d], Jizheng Duan[bc], Changwei Hao[bc], Yuan Tian[bc], Wenshan Duan[a], Lei Yang[bce], Ping Lin[*f] and Sheng Zhang[*d]

[a]College of Physics and Electronic Engineering, Northwest Normal University, Lanzhou 730070, China

[b]Advanced Energy Science and Technology Guangdong Laboratory, Huizhou 516000, China

[c]Institute of Modern Physics, Chinese Academy of Science, Lanzhou 730000, China

[d]Center for Basic Teaching and Experiment, Nanjing University of Science and Technology, Jiangyin 214443, China

[e]School of Nuclear Science and Technology, University of Chinese Academy of Science, Beijing 100043, China

[f]School of Intelligent Manufacturing, Weifang University of Science and Technology, Weifang, 262700, China

Supplementary Text

We performed additional stability analyses and referenced recent studies[1], which explores the stability of point defects in 2D materials. Specifically, we employed AIMD simulations to evaluate the thermal stability of the system. Figure S20 shows the fluctuations of total potential energy for V_{Ba}, V_{Ag}, V_{Bi}, and BaAgBi at 300 K and 500 K temperatures. Throughout the simulations, the atoms exhibited only slight vibrations around their equilibrium positions, indicating that the material remains stable within the temperature range considered in our study.

Supplementary Figures

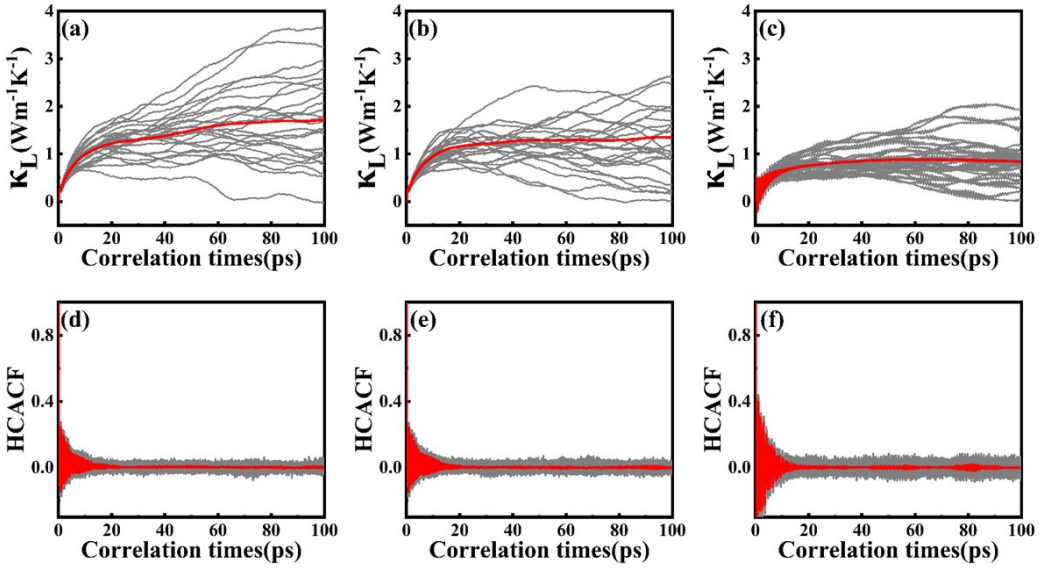

Figure S1. The lattice thermal conductivity for BaAgBi at 300 K along the (a) a-, (b) b-, and (c) c-axes. Normalized heat current autocorrelation function (HCACF) for 25 independent MD simulations at 300 K along the (d) a-, (e) b-, and (f) c-axes. The gray lines represent the thermal conductivity from 25 independent simulations, while the red solid line indicates the corresponding average value.

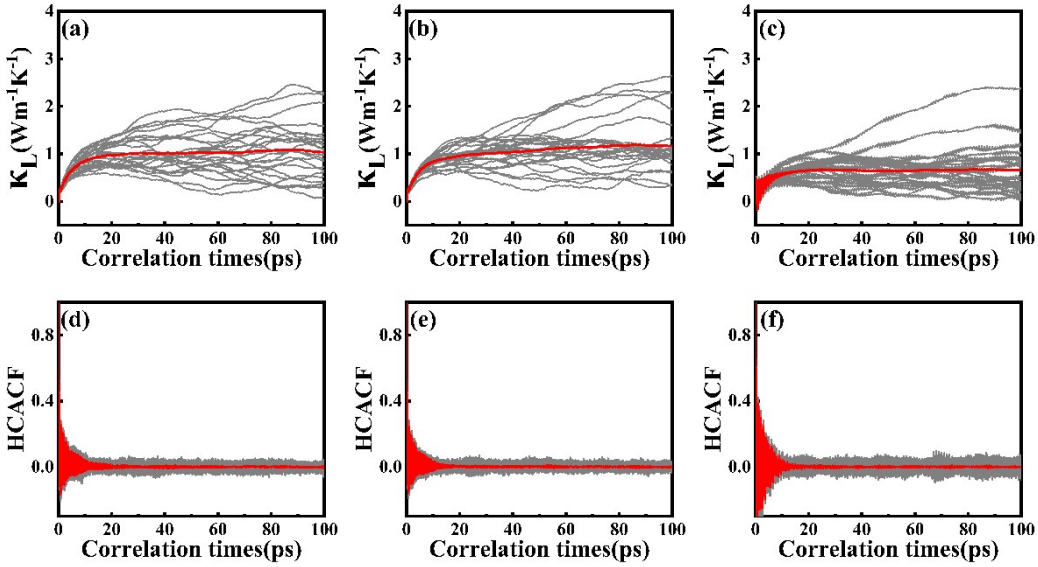

Figure S2. The lattice thermal conductivity for V_{Ba} (vacancy concentration (0.1%)) at 300 K along the (a) a-, (b) b-, and (c) c-axes. Normalized heat current autocorrelation function (HCACF) for 25 independent MD simulations at 300 K along the (d) a-, (e) b-, and (f) c-axes. The gray lines represent the thermal conductivity from 25 independent simulations, while the red solid line indicates the corresponding average value.

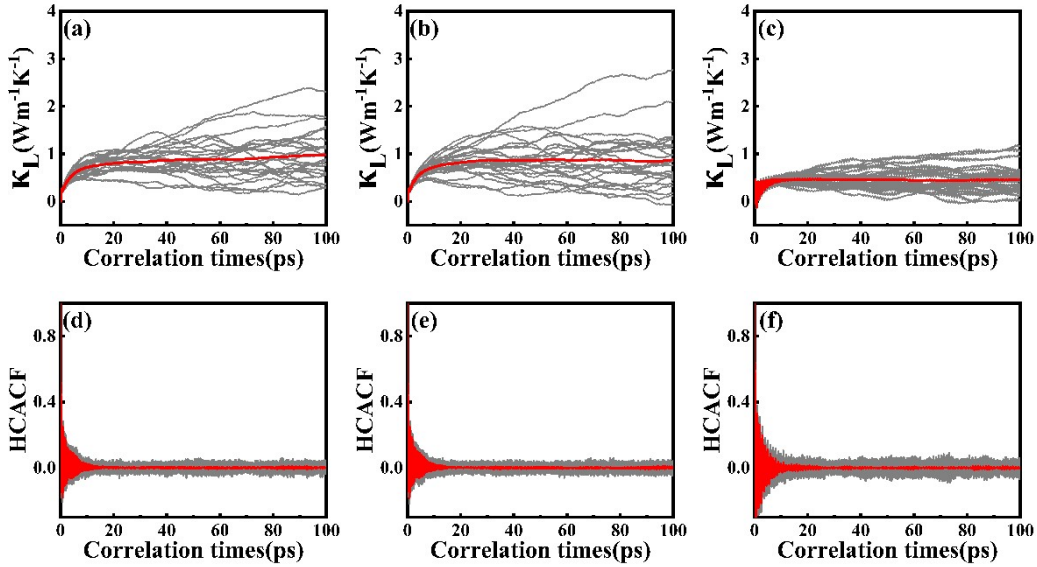

Figure S3. The lattice thermal conductivity for V_{Ba} (vacancy concentration (0.3%)) at 300 K along the (a) a-, (b) b-, and (c) c-axes. Normalized heat current autocorrelation

function (HCACF) for 25 independent MD simulations at 300 K along the (d) a-, (e) b-, and (f) c-axes. The gray lines represent the thermal conductivity from 25 independent simulations, while the red solid line indicates the corresponding average value.

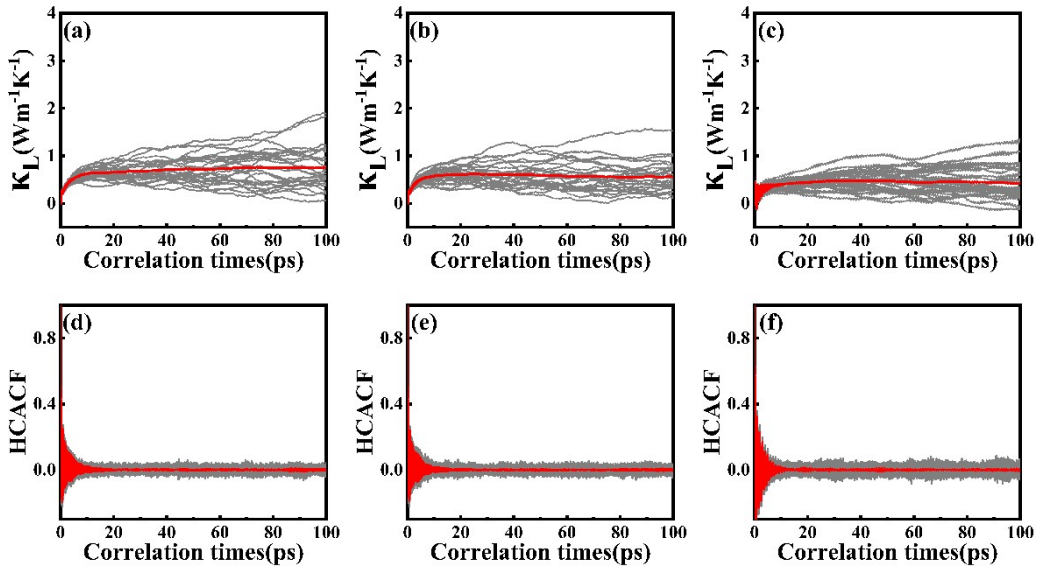

Figure S4. The lattice thermal conductivity for V_{Ba} (vacancy concentration (0.5%)) at 300 K along the (a) a-, (b) b-, and (c) c-axes. Normalized heat current autocorrelation function (HCACF) for 25 independent MD simulations at 300 K along the (d) a-, (e) b-, and (f) c-axes. The gray lines represent the thermal conductivity from 25 independent simulations, while the red solid line indicates the corresponding average value.

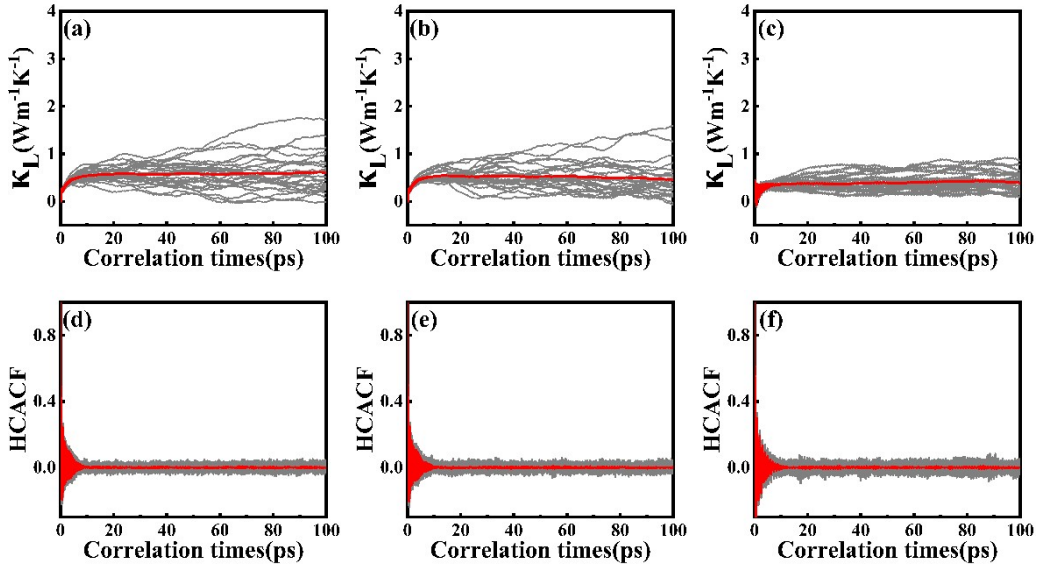

Figure S5. The lattice thermal conductivity for V_{Ba} (vacancy concentration (0.7%)) at 300 K along the (a) a-, (b) b-, and (c) c-axes. Normalized heat current autocorrelation function (HCACF) for 25 independent MD simulations at 300 K along the (d) a-, (e) b-, and (f) c-axes. The gray lines represent the thermal conductivity from 25

independent simulations, while the red solid line indicates the corresponding average value.

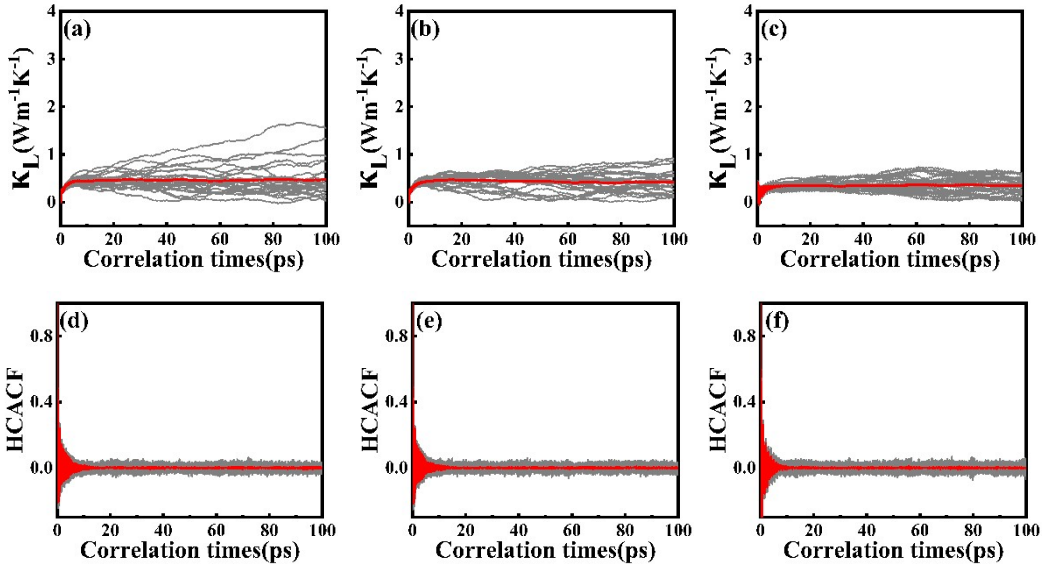

Figure S6. The lattice thermal conductivity for V_{Ba} (vacancy concentration (0.9%)) at 300 K along the (a) a-, (b) b-, and (c) c-axes. Normalized heat current autocorrelation function (HCACF) for 25 independent MD simulations at 300 K along the (d) a-, (e) b-, and (f) c-axes. The gray lines represent the thermal conductivity from 25 independent simulations, while the red solid line indicates the corresponding average value.

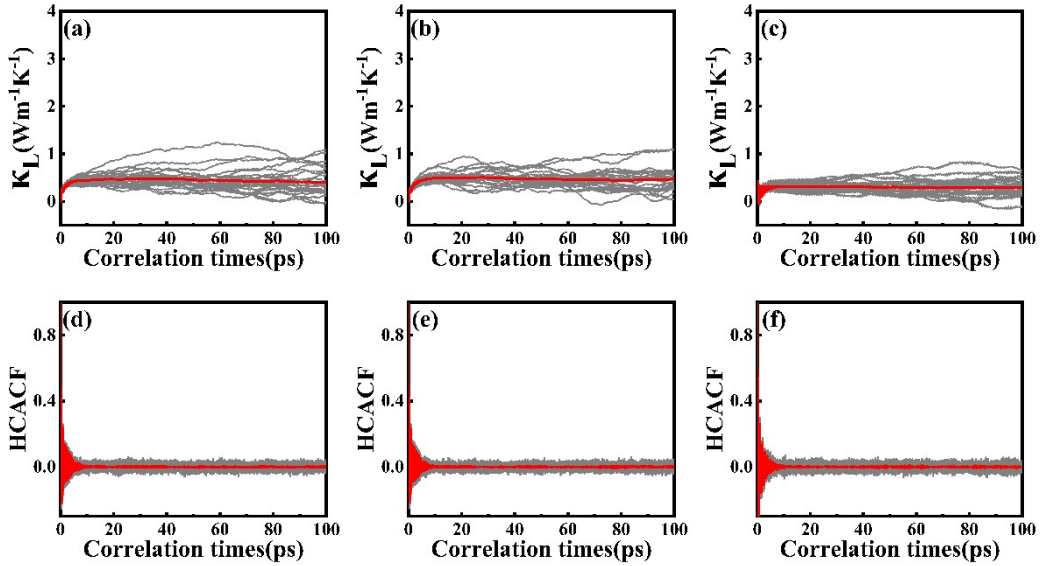

Figure S7. The lattice thermal conductivity for V_{Ba} (vacancy concentration (1.0%)) at 300 K along the (a) a-, (b) b-, and (c) c-axes. Normalized heat current autocorrelation function (HCACF) for 25 independent MD simulations at 300 K along the (d) a-, (e) b-, and (f) c-axes. The gray lines represent the thermal conductivity from 25 independent simulations, while the red solid line indicates the corresponding average value.

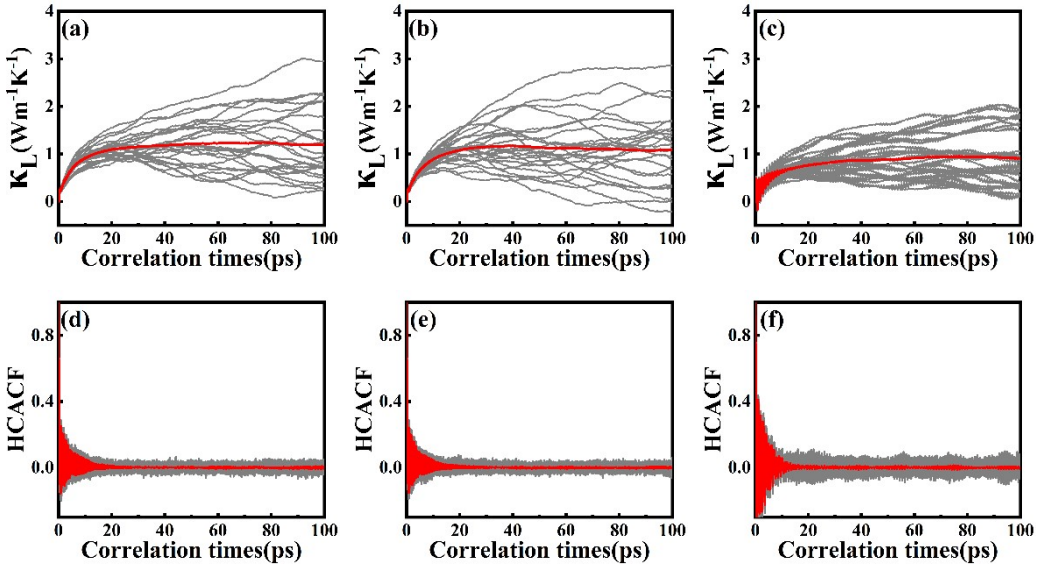

Figure S8. The lattice thermal conductivity for V_{Ag} (vacancy concentration (0.1%)) at 300 K along the (a) a-, (b) b-, and (c) c-axes. Normalized heat current autocorrelation function (HCACF) for 25 independent MD simulations at 300 K along the (d) a-, (e) b-, and (f) c-axes. The gray lines represent the thermal conductivity from 25 independent simulations, while the red solid line indicates the corresponding average value.

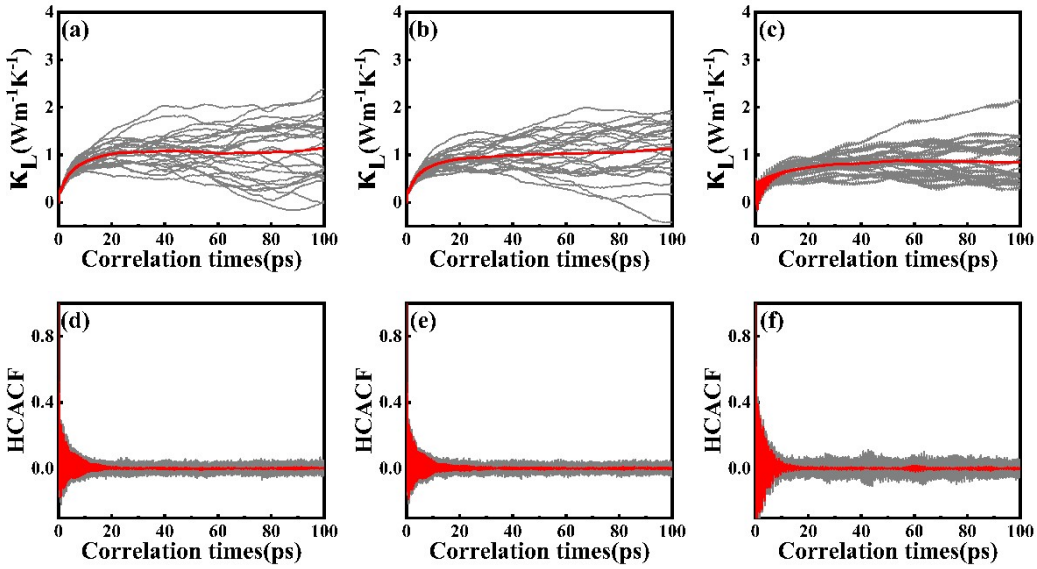

Figure S9. The lattice thermal conductivity for V_{Ag} (vacancy concentration (0.3%)) at 300 K along the (a) a-, (b) b-, and (c) c-axes. Normalized heat current autocorrelation function (HCACF) for 25 independent MD simulations at 300 K along the (d) a-, (e) b-, and (f) c-axes. The gray lines represent the thermal conductivity from 25 independent simulations, while the red solid line indicates the corresponding average value.

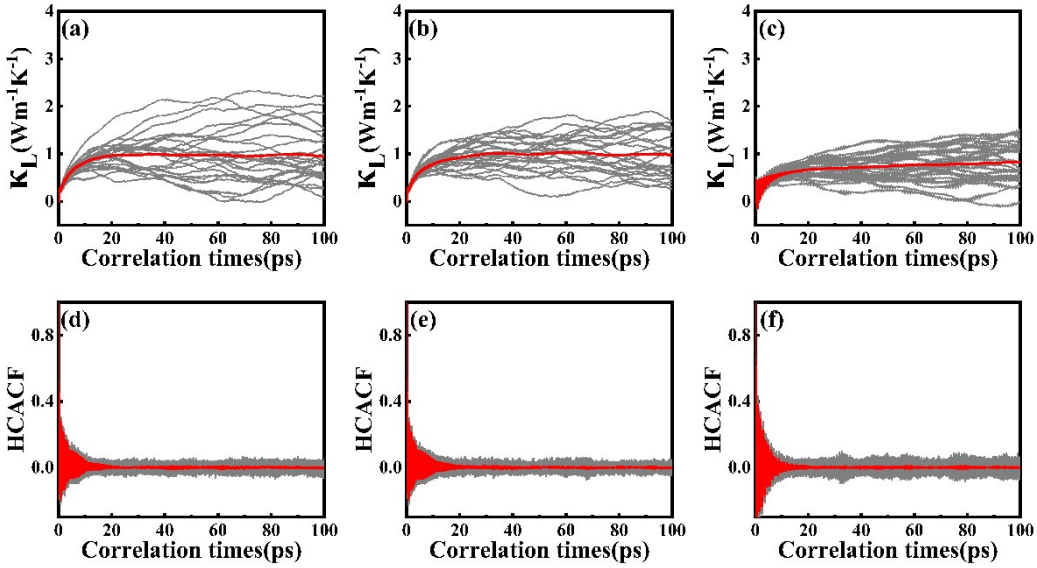

Figure S10. The lattice thermal conductivity for V_{Ag} (vacancy concentration (0.5%)) at 300 K along the (a) a-, (b) b-, and (c) c-axes. Normalized heat current autocorrelation function (HCACF) for 25 independent MD simulations at 300 K along the (d) a-, (e) b-, and (f) c-axes. The gray lines represent the thermal conductivity from 25 independent simulations, while the red solid line indicates the corresponding average value.

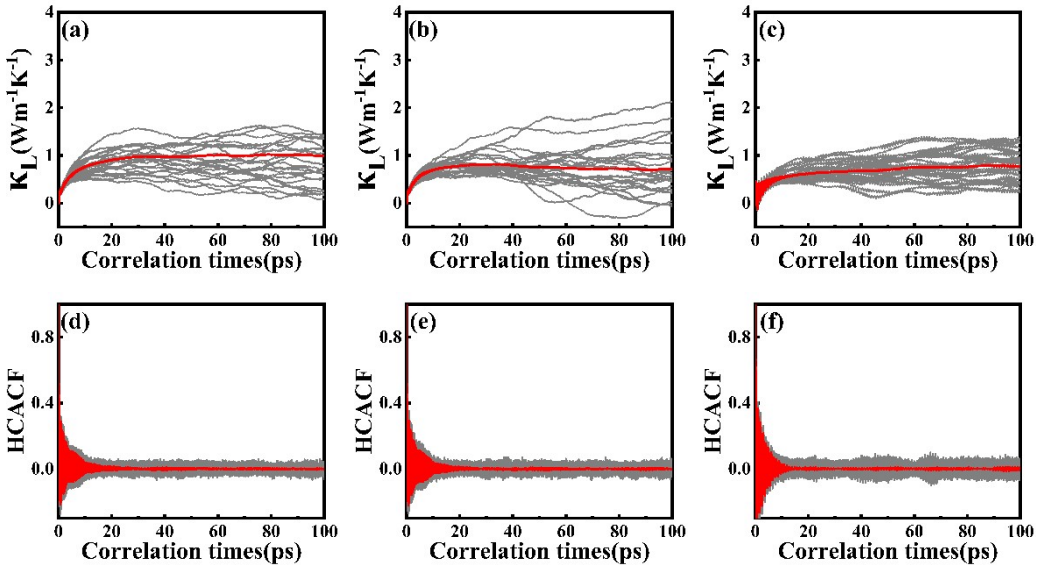

Figure S11. The lattice thermal conductivity for V_{Ag} (vacancy concentration (0.7%)) at 300 K along the (a) a-, (b) b-, and (c) c-axes. Normalized heat current autocorrelation function (HCACF) for 25 independent MD simulations at 300 K along the (d) a-, (e) b-, and (f) c-axes. The gray lines represent the thermal conductivity from 25 independent simulations, while the red solid line indicates the corresponding average value.

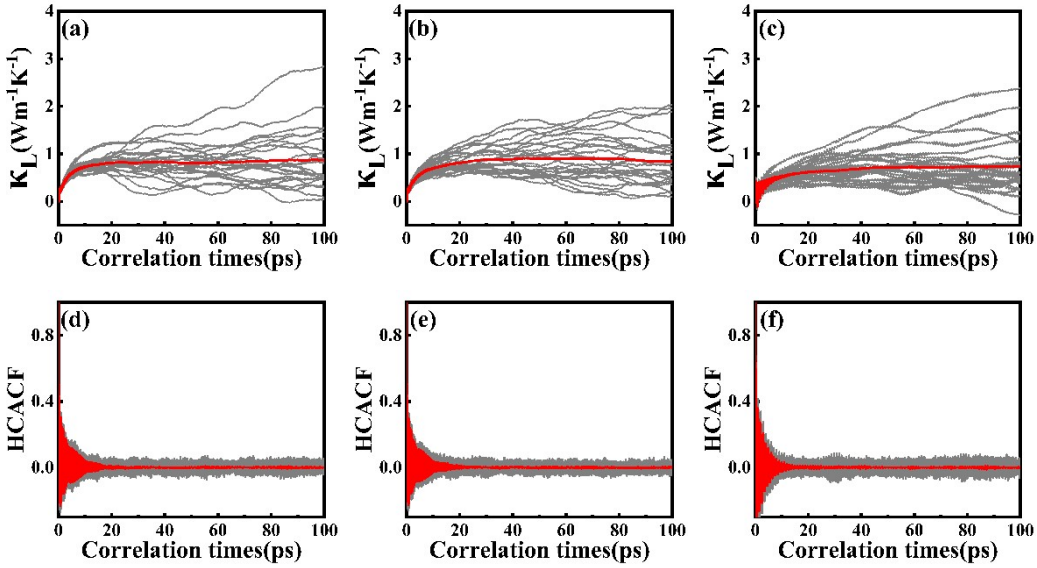

Figure S12. The lattice thermal conductivity for V_{Ag} (vacancy concentration (0.9%)) at 300 K along the (a) a-, (b) b-, and (c) c-axes. Normalized heat current autocorrelation function (HCACF) for 25 independent MD simulations at 300 K along the (d) a-, (e) b-, and (f) c-axes. The gray lines represent the thermal conductivity from 25 independent simulations, while the red solid line indicates the corresponding average value.

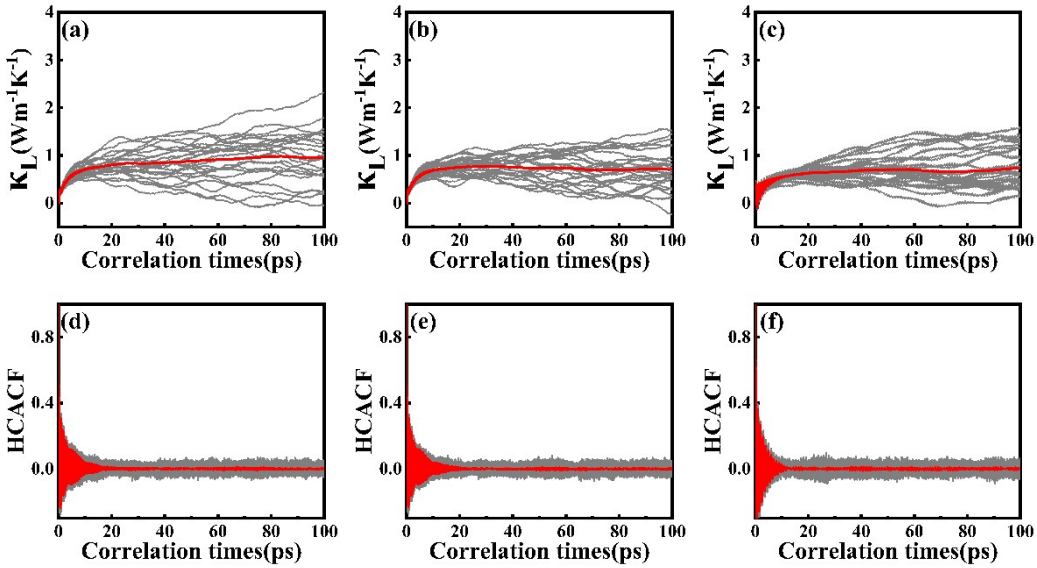

Figure S13. The lattice thermal conductivity for V_{Ag} (vacancy concentration (1.0%)) at 300 K along the (a) a-, (b) b-, and (c) c-axes. Normalized heat current autocorrelation function (HCACF) for 25 independent MD simulations at 300 K along the (d) a-, (e) b-, and (f) c-axes. The gray lines represent the thermal conductivity from 25 independent simulations, while the red solid line indicates the corresponding average value.

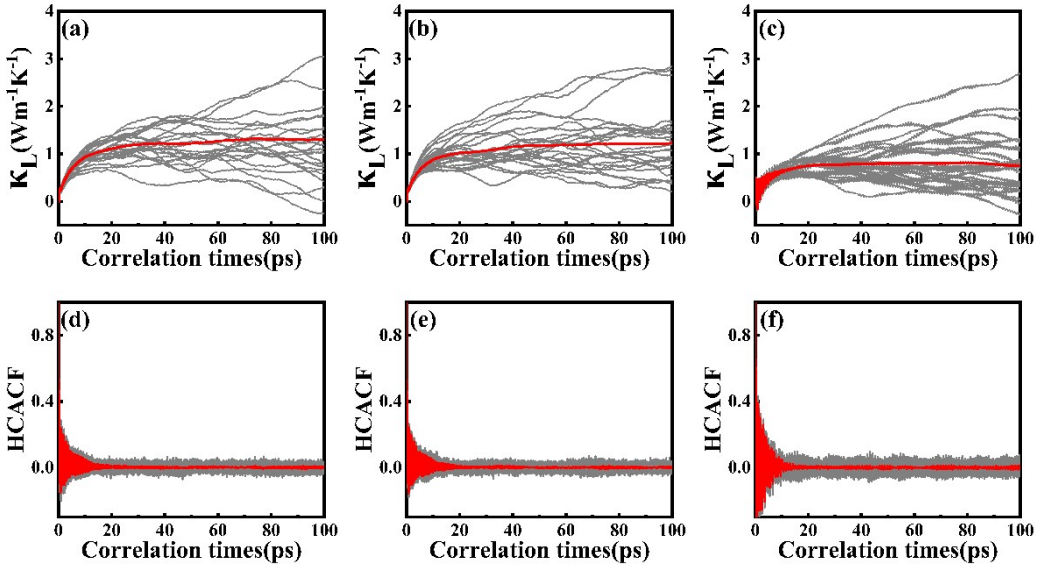

Figure S14. The lattice thermal conductivity for V_{Bi} (vacancy concentration (0.1%)) at 300 K along the (a) a-, (b) b-, and (c) c-axes. Normalized heat current autocorrelation function (HCACF) for 25 independent MD simulations at 300 K along the (d) a-, (e) b-, and (f) c-axes. The gray lines represent the thermal conductivity from 25 independent simulations, while the red solid line indicates the corresponding average value.

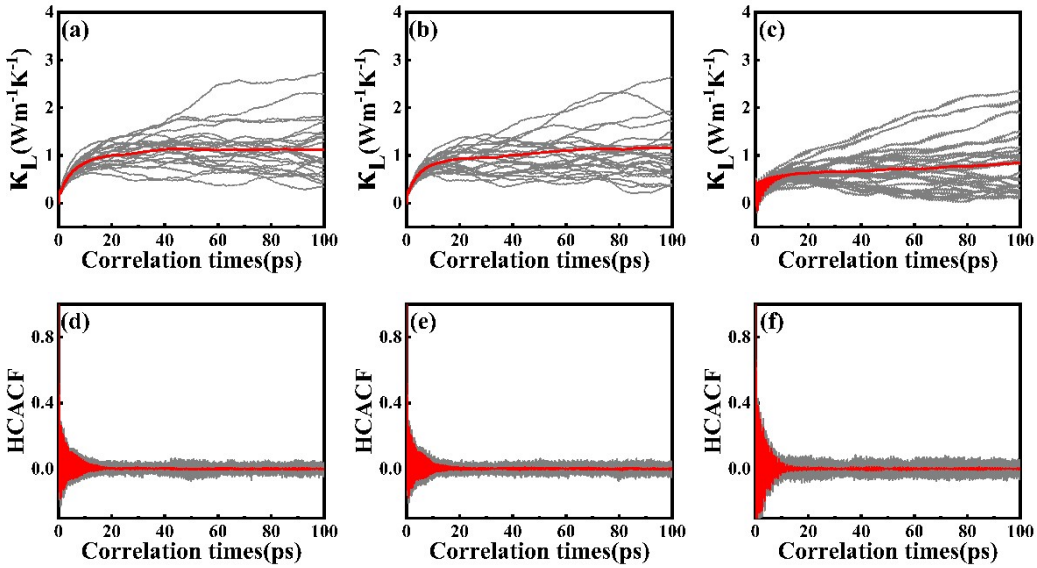

Figure S15. The lattice thermal conductivity for V_{Bi} (vacancy concentration (0.3%)) at 300 K along the (a) a-, (b) b-, and (c) c-axes. Normalized heat current autocorrelation function (HCACF) for 25 independent MD simulations at 300 K along the (d) a-, (e) b-, and (f) c-axes. The gray lines represent the thermal conductivity from 25 independent simulations, while the red solid line indicates the corresponding average value.

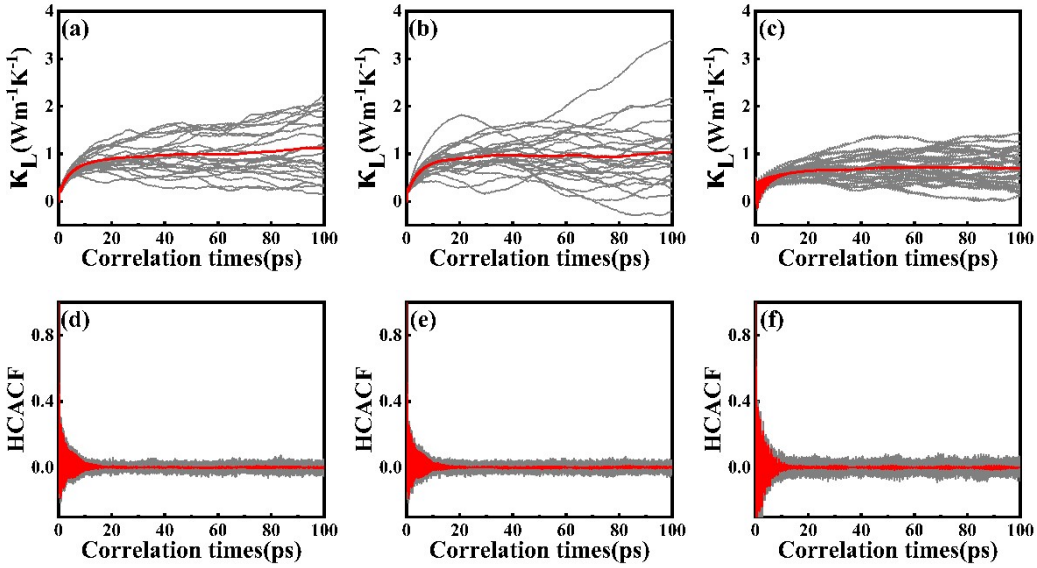

Figure S16. The lattice thermal conductivity for V_{Bi} (vacancy concentration (0.5%)) at 300 K along the (a) a-, (b) b-, and (c) c-axes. Normalized heat current autocorrelation function (HCACF) for 25 independent MD simulations at 300 K along the (d) a-, (e) b-, and (f) c-axes. The gray lines represent the thermal conductivity from 25 independent simulations, while the red solid line indicates the corresponding average value.

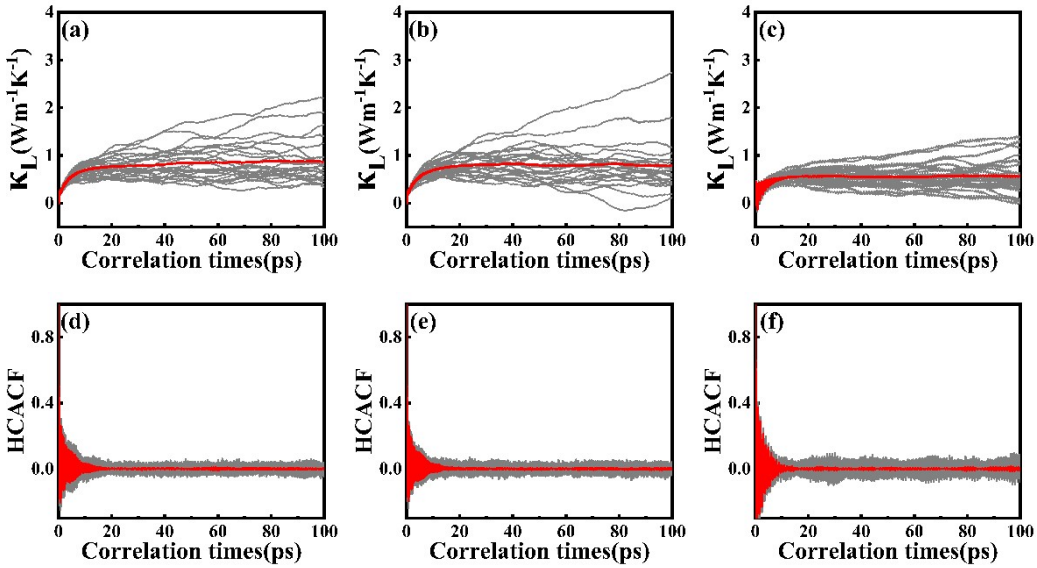

Figure S17. The lattice thermal conductivity for V_{Bi} (vacancy concentration (0.7%)) at 300 K along the (a) a-, (b) b-, and (c) c-axes. Normalized heat current autocorrelation function (HCACF) for 25 independent MD simulations at 300 K along the (d) a-, (e) b-, and (f) c-axes. The gray lines represent the thermal conductivity from 25 independent simulations, while the red solid line indicates the corresponding average value.

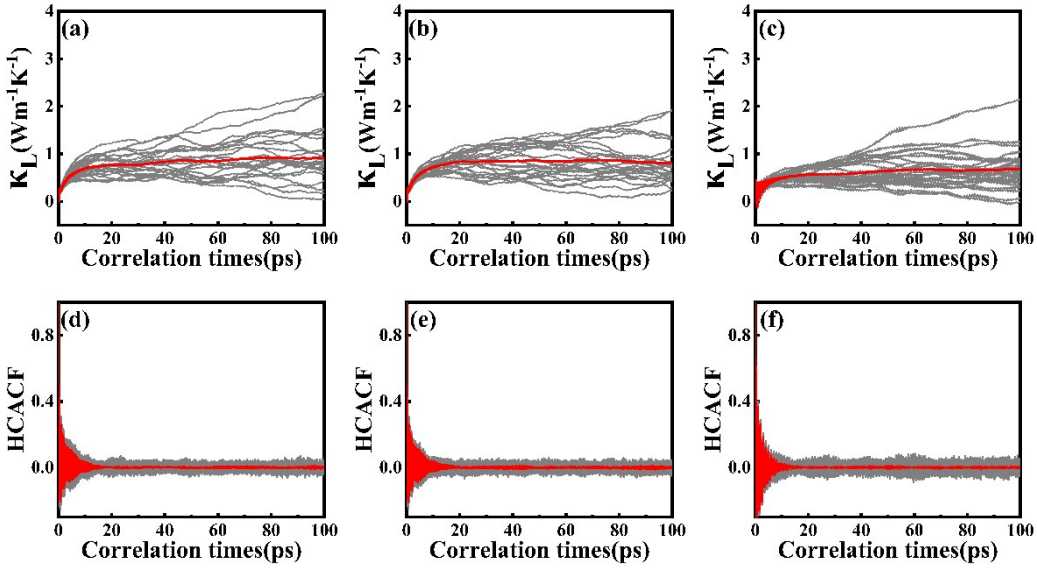

Figure S18. The lattice thermal conductivity for V_{Bi} (vacancy concentration (0.9%)) at 300 K along the (a) a-, (b) b-, and (c) c-axes. Normalized heat current autocorrelation function (HCACF) for 25 independent MD simulations at 300 K along the (d) a-, (e) b-, and (f) c-axes. The gray lines represent the thermal conductivity from 25 independent simulations, while the red solid line indicates the corresponding average value.

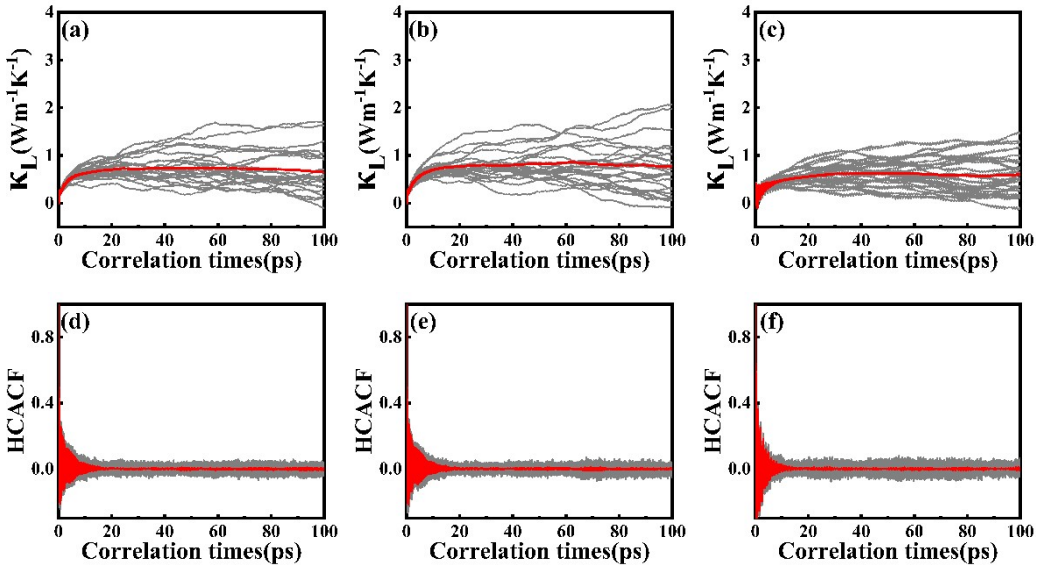

Figure S19. The lattice thermal conductivity for V_{Bi} (vacancy concentration (1.0%)) at 300 K along the (a) a-, (b) b-, and (c) c-axes. Normalized heat current autocorrelation function (HCACF) for 25 independent MD simulations at 300 K along the (d) a-, (e) b-, and (f) c-axes. The gray lines represent the thermal conductivity from 25 independent simulations, while the red solid line indicates the corresponding average value.

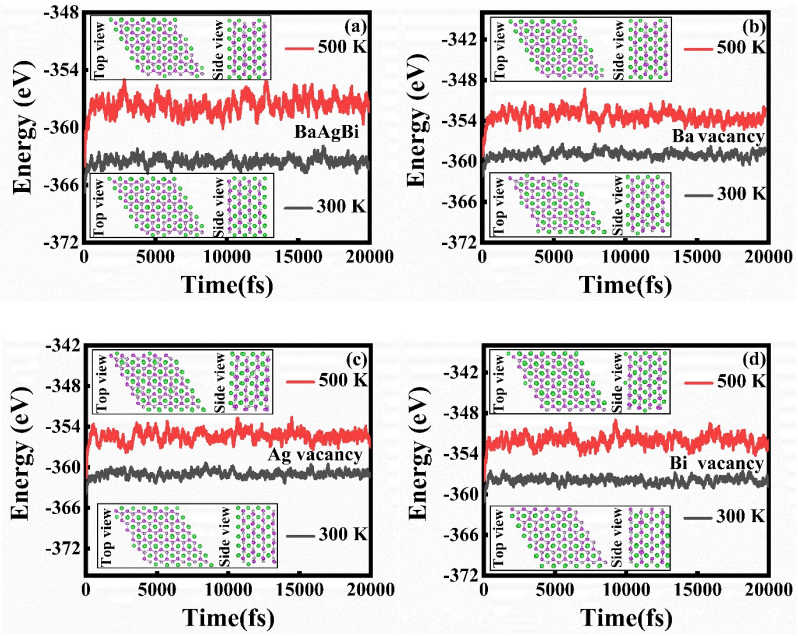

Figure S20. Total energy for (a)BaAgBi (108-atom), (b) BaAgBi with Ba vacancy defect, (c) BaAgBi with Ba vacancy defect, and (d) BaAgBi with Bi vacancy defect (107 atoms) at different temperatures during AIMD simulation.

References

1. Q. Gui, Z. Wang and Z. Zhang, Chemistry of Materials: A Publication of the American Chemistry Society, 2023.